

Pseudo-Topochemical Synthesis of α -Fe in Aqueous Solution Using an Aluminum Matrix

A. F. Dresvyannikov and M. E. Kolpakov

Kazan State University of Technology, Kazan, Tatarstan, Russia

Received May 20, 2003

Abstract—Processes occurring in synthesis of α -Fe from a Fe(III) solution using an aluminum matrix were studied. The reaction kinetics strongly depends on the state of the matrix.

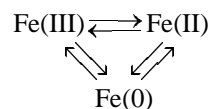
Dispersed and ultradispersed iron metal and its alloys are widely used in various branches of science and engineering thanks to their unique magnetic, mechanical, catalytic, and other properties. The properties of these materials largely depend on the procedure of their preparation. It should be noted that the known processes for reduction of Fe(III) from aqueous solutions are very few and often do not ensure high yield of iron metal under normal conditions. Also, it is known that the history of iron metal preparation appreciably affects its physical and chemical properties, which should be taken into account in preparation of materials with preset characteristics.

Metal formulations with an aluminum matrix attract much researchers' attention [1–5]. Thanks to a unique combination of protective properties of surface oxide–hydroxide layers and intrinsic chemical activity, aluminum under definite conditions chemically reacts with the surrounding medium to form compounds exhibiting a series of specific properties [6, 7]. According to numerous papers, finely dispersed aluminum powder considerably surpasses compact aluminum in the chemical activity toward water and aqueous solutions of various compounds [8, 9]. It is believed [6, 8, 9] that this is due to the developed surface of the powders, to strongly defective state of the surface oxide–hydroxide films on fine particles, and to strong heat-up of the solid phase in the course of oxidation [9]. These factors can appreciably affect the course and extent of the reaction of finely dispersed and compact aluminum with an aqueous solution containing metal ions. It should be noted, however, that we found no detailed information on the reduction of Fe(III) ions with aluminum in solution. In this connection, it seems important to study how the aluminum matrix affects the redox process involving reduction of Fe(III).

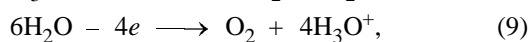
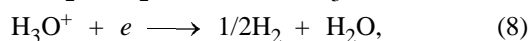
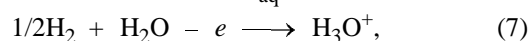
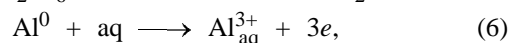
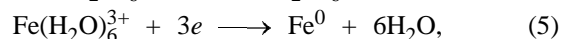
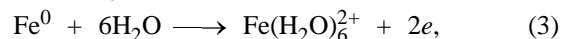
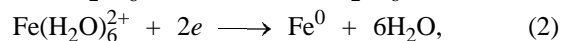
Our goal was to elucidate the mechanism of the

reaction of compact and dispersed (with different particle size) aluminum with an aqueous solution of Fe(III) chloride and to reveal characteristic kinetic features of separate steps of the process.

We found previously that Fe(III) in aqueous solution is reduced on a dispersed aluminum matrix in two steps: Fe(III) \rightarrow Fe(II) \rightarrow Fe(0) [10]. Since the reduction of Fe(III) yields two products, Fe(II) and Fe(0), a question arises: What is the sequence of transformations in the system? The tentative scheme of redox transformations of Fe(III) in its reaction with aluminum is as follows.



The reactions in such solutions are complicated by complexation of the oxidized and reduced iron species and their blocking with ligands and solvent molecules. The results of our preliminary experiments, in combination with published data on redox reactions involving iron ions [11, 12], suggest the occurrence of the following steps (at pH 0.5):



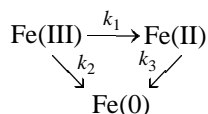
Since the equilibrium potential of the reduced iron

is more negative than the potential of the equilibrium hydrogen electrode at this pH, the metal can dissolve by the reaction $\text{Fe}^0 + 2\text{H}_3\text{O}^+ = \text{Fe}_{\text{aq}}^{2+} + \text{H}_2 + 2\text{H}_2\text{O}$ [12]. The presence of dissolved oxygen in the electrolyte makes probable the occurrence of reaction (10), which, when conjugated with reaction (3), will cause appreciable dissolution of the deposited iron. Along with reaction (2), several other reactions (e.g., redox processes of liberation–ionization of hydrogen or reduction–liberation of oxygen) are also possible on contact of the deposited iron with a solution of iron salts. However, in this case the rates of reactions (7)–(10) will be very low compared to the rates of reactions (2) and (3).

To elucidate the mechanism of Fe(III) reduction, we used the method of relative selectivity [13, 14]. The relative selectivity γ is the ratio of the selectivities S with respect to reaction products, or the ratio of the degrees of conversion of the starting reactant into the products [13]. To determine the relative contributions of the parallel and consecutive pathways of formation of reaction products, it is sufficient to determine the relative selectivity at a short reaction time.

We showed previously [15] that, with aluminum foil as reductant, the relative selectivity of the process $\gamma \neq 0$, which suggests concurrent formation of Fe(II) and Fe(0) from Fe(III). A similar calculation for the case of reduction of Fe(III) with dispersed aluminum showed that γ tends to zero (evidence for the consecutive reaction).

These results allow us to suggest a general scheme of the reaction of Fe(III) ions with aluminum, both compact and dispersed with various particle size:



where k_1 , k_2 , and k_3 are the rate constants of the corresponding reactions, s^{-1} .

The overall process can be described by a system of kinetic equations (11)–(13):

$$[\text{Fe(III)}] = [\text{Fe(III)}]_0 \exp[-(k_1 + k_2)t], \quad (11)$$

$$[\text{Fe(0)}] = [\text{Fe(III)}]_0 \left[\frac{k_2}{k_1 + k_2} \{1 - \exp[-(k_1 + k_2)t]\} + \left(-\frac{k_3}{k_3 - k_1} \exp(-k_1 t) + \frac{k_1}{k_3 - k_1} \exp(-k_3 t) \right) \right], \quad (12)$$

$$[\text{Fe(II)}] = [\text{Fe(III)}]_0 - [\text{Fe(III)}] - [\text{Fe(0)}]$$

$$\text{or} \\ [\text{Fe(II)}] = [\text{Fe(III)}]_0 \left[1 - \exp[-(k_1 + k_2)t] - \frac{k_2}{k_1 + k_2} \{1 - \exp[-(k_1 + k_2)t]\} - \left(1 - \frac{k_3}{k_3 - k_1} \exp(-k_1 t) + \frac{k_1}{k_3 - k_1} \exp(-k_3 t) \right) \right], \quad (13)$$

where $[\text{Fe(III)}]_0$ is the initial Fe(III) concentration, M; $[\text{Fe(III)}]$, $[\text{Fe(II)}]$, and $[\text{Fe(0)}]$ are the running concentrations of Fe(III), Fe(II), and Fe(0), respectively, M; and t is the time, s.

Since Fe(0) occurs in the nonionic state, $[\text{Fe(0)}]$ can be replaced by $m[\text{Fe(0)}]$:

$$\alpha = \frac{m[\text{Fe(0)}]}{m_0[\text{Fe(III)}]} = \frac{k_2}{k_1 + k_2} \{1 - \exp[-(k_1 + k_2)t]\} + \left[1 - \frac{k_3}{k_3 - k_1} \exp(-k_1 t) + \frac{k_1}{k_3 - k_1} \exp(-k_3 t) \right]. \quad (14)$$

where α is the yield of Fe(0); $m[\text{Fe(0)}]$, weight of Fe(0), g; $m_0[\text{Fe(III)}]$, weight of the starting Fe(III), g.

Two limiting cases can be considered.

(1) $k_3 \rightarrow 0$. In this case, from Eqs. (13) and (14) we obtain the following expressions:

$$[\text{Fe(II)}] = [\text{Fe(III)}]_0 \frac{k_1}{k_1 + k_2} \{1 - \exp[-(k_1 + k_2)t]\}, \quad (15)$$

$$\alpha = \frac{m[\text{Fe(0)}]}{m_0[\text{Fe(III)}]} = \frac{k_2}{k_1 + k_2} \{1 - \exp[-(k_1 + k_2)t]\}. \quad (16)$$

These equations correspond to formation of Fe(II) and Fe(0), i.e., Fe(0) is formed concurrently with Fe(II) [Eq. (5)], with the contribution of the consecutive pathway being negligible. This is the case at a small specific surface area of the aluminum matrix, characteristic of the compact metal ($S_{\text{sp}} < 100 \text{ cm}^2 \text{ g}^{-1}$, Fig. 1a).

(2) $k_2 \rightarrow 0$. For this case, from Eqs. (11), (13), and (14) we obtain Eqs. (17)–(19), respectively.

$$[\text{Fe(III)}] = [\text{Fe(III)}]_0 \exp[-(k_1)t], \quad (17)$$

$$[\text{Fe(II)}] = [\text{Fe(III)}]_0 \frac{k_1}{k_1 + k_2} [\exp(-k_1 t) - \exp(-k_3 t)], \quad (18)$$

$$\alpha = \frac{m[\text{Fe(0)}]}{m_0[\text{Fe(III)}]} = 1 - \frac{k_3}{k_3 - k_1} \exp(-k_1 t) + \frac{k_1}{k_3 - k_1} \exp(-k_3 t). \quad (19)$$

At a sufficiently large specific surface area ($S_{\text{sp}} > 200 \text{ cm}^2 \text{ g}^{-1}$), Fe(0) is formed by the consecutive

pathway [Eq. (2)], with the contribution of the parallel pathway being negligible. This case is illustrated graphically in Fig. 1b.

In a certain "transition" region (tentative range $100 < S_{sp} < 200 \text{ cm}^3 \text{ g}^{-1}$), $k_2 \approx k_3$, i.e., Fe(0) is formed by a mixed parallel-consecutive mechanism with a comparable contribution of the two alternative pathways (Fig. 1c).

In all these cases, the results of calculations with the suggested model reasonably agree with the experimental data (Figs. 1a–1c). The kinetic curves of Fe(0) deposition, α – τ , have a shape typical of topochemical reactions with a pronounced induction period and steps of reaction development and deceleration. The reaction is accompanied by a fairly strong heat evolution. Lyashko *et al.* [9] considered the heat-up of aluminum particles and their aggregates upon their reaction with water. According to their estimates, under the adiabatic conditions the heat release from the reaction of two or three Al monolayers is sufficient to heat a particle 0.1 μm in diameter to the melting point (according to the experimental data, the reaction rate is 0.5–1.5 monolayers per second). With the heat exchange taken into account, the estimated heat-up is of the order of hundreds degrees. This considerable increase in the particle temperature causes apparent rate constant of the reaction to increase, which results in progressing heat-up. The reaction becomes controlled by external diffusion, and the temperature of the particles being oxidized reaches a maximum. A characteristic evidence for this transition is a portion in the kinetic curve, in which the reaction rate is maximal and constant in a wide range of α .

The processes under consideration can be described taking into account differences in the structure and physicochemical properties of the surface oxide layer in compact and dispersed aluminum [16, 17]. Experiments performed in various media show that aluminum occurs in the passive state even in aggressive aqueous solutions [16, 18]. The oxide film on aluminum microparticles, compared to that on the compact metal, is nonuniform and rough, with a fine relief in the form of folds, pits, and prominences; it is an amorphous matrix of aluminum oxide with inclusions of very fine γ - Al_2O_3 crystallites; traces of crystalline mono- and trihydrates of aluminum oxide were revealed [17]. The surface layers also contain ultramicroamounts of a foreign phase (e.g., Si, Fe, Zn, K, Mg, etc.).

It is also known that the crystalline oxide forming in dry air or after high-temperature heating of Al powders extends the metal lattice at room temperature and contracts it on heating [19]. The arising tangential

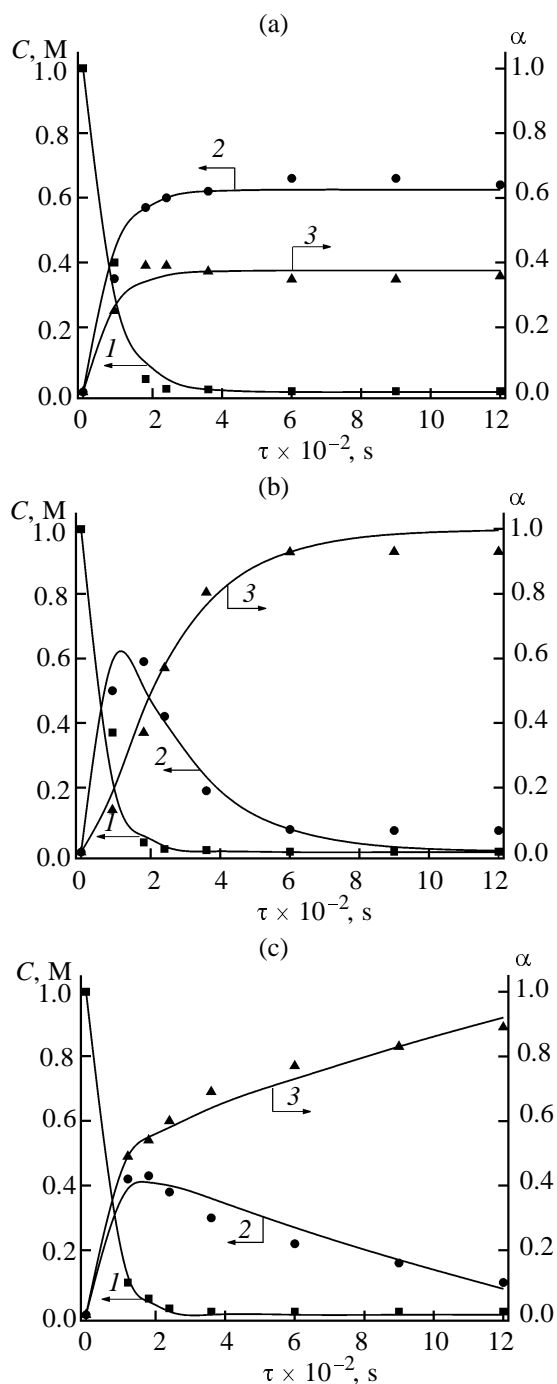


Fig. 1. Kinetic curves of reduction of Fe(III) ions in aqueous solution: (1) Fe(III), (2) Fe(II), and (3) Fe(0). Data for (a) A-999 Al foil, (b) Al particles of size $85 \pm 15 \mu\text{m}$, and (c) Al particles of size $175 \pm 55 \mu\text{m}$; 298 K, 1.0 M FeCl_3 , pH 0.5; points are experimental data, and lines are calculation results.

stresses, which are more or less uniformly distributed over the particle volume, are due to differences in the structure and thermal expansion of aluminum metal and its oxide [20]. As a result, the microstructure of

Characteristics of the crystal lattice of dispersed Al and reduced Fe, determined by X-ray diffraction analysis

| Miller indices | | | Interplanar spacing, Å | Crystallite size, Å | Micro-stress |
|----------------|----------|----------|------------------------|---------------------|--------------|
| <i>h</i> | <i>k</i> | <i>l</i> | | | |
| Dispersed Al | | | | | |
| 1 | 1 | 1 | 2.3375 | 1092 | 2.0863 |
| 2 | 0 | 0 | 2.0244 | 1616 | 5.9230 |
| 2 | 2 | 0 | 1.4314 | 1223 | 1.7823 |
| 3 | 1 | 1 | 1.2207 | 1369 | 1.3656 |
| 2 | 2 | 2 | 1.1688 | 1092 | 2.0863 |
| 4 | 0 | 0 | 1.0122 | 1616 | 5.9230 |
| Reduced Fe | | | | | |
| 1 | 1 | 0 | 2.0268 | 534 | 0.0029 |
| 2 | 0 | 0 | 1.4332 | 370 | 0.0042 |
| 2 | 1 | 1 | 1.1702 | 534 | 0.0029 |
| 2 | 2 | 0 | 1.0134 | 534 | 0.0029 |

the surface of the oxide layer on Al particles is characterized by numerous microcracks whose formation is caused by high stresses in the oxide shells, due to considerable differences in the molar volumes of the metal and oxide and to different densities of the amorphous and crystalline oxides [16, 20]. Furthermore, the oxide shells on particles have numerous structural defects. It should be noted also that powders whose particles are coated with a crystalline surface film are oxidized more intensely than those coated with the amorphous oxide [21]. These features of compact and dispersed aluminum determine the specific features of their reaction with a solution containing Fe(III) ions.

The Cl^- ions released in dissolution of FeCl_3 are depassivators displacing or partially substituting, by the adsorption mechanism, the passivating oxygen in the surface film to form a surface complex [22] capable of subsequently passing into the solution. Also, aggressive ions can directly contact the metal surface as a result of mechanical degradation of the oxide

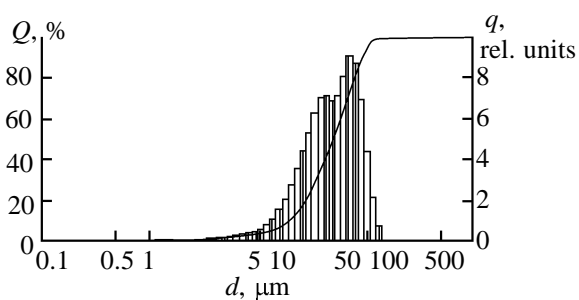


Fig. 2. Particle-size distribution of α -Fe: (Q) integral (curve) and (q) differential (histogram).

layer [23]. Oxidation of aluminum is accompanied by reduction of proton donors (hydrogen depolarization) and of the oxidant (iron ions). The latter process, as shown above, is intricate (it occurs in one or two steps depending on the extent of dispersion of the aluminum matrix) and yields a Fe(0) precipitate as the final product. After appearance of a layer of iron metal, hydrogen liberation becomes more intense. However, the rate of this process is appreciably (by approximately three orders of magnitude) lower than the rate of the deposition of iron metal [15].

The particle-size distribution of iron powders obtained using a close-cut fraction of dispersed Al (71–100 μm) is shown in Fig. 2. It is seen that the narrow particle-size distribution of the powder is preserved. The Fe(0) deposit is formed on the surface of Al particles with preservation of the shape and size of the initial matrix, i.e., dissolution of Al and formation of spherical nuclei of Fe metal occur simultaneously. With time, Al is mostly dissolved, and the forming Fe particle is virtually a polar sphere with a large number of spherical subparticles on the surface, of pores, and of thread-like nuclei inside the pores (Fig. 3). This is also indirectly suggested by the bulk density, which is abnormally low for iron powders (1.25 g cm^{-3}). It should be noted that the deposition of Fe on the Al particles is nonuniform, i.e., in any stage of the reaction, particles fully covered with the deposit coexist with unchanged particles.

Since deposition of Fe may be accompanied by formation of its basic compounds, it is appropriate to determine the qualitative and quantitative composition of the deposits formed on the Al matrix. According to X-ray phase analysis and local microanalysis, the samples obtained from dispersed Al ($85 \pm 15\text{-}\mu\text{m}$ fraction) are mechanical mixtures of α -Fe and Al crystals (Fig. 4, pattern 1). After keeping the deposit in 3.0 M NaOH, only the α -Fe phase was detected (Fig. 4, pattern 2). Without alkali treatment, an amorphous phase (presumably pseudoboehmite) gradually appears, which is followed by formation of bayerite crystals formed from metastable products of aluminum dissolution.

From the X-ray diffraction data, using the MAUD software, we determined the Miller indices of the initial Al and of the synthesized Fe and calculated the sizes of the coherent scattering domains and the microstresses (see table). Also, with the MAUD software, we obtained an image of an α -Fe crystallite (Fig. 5). It has the shape of a cube with smoothed edges; axis (100) is directed toward the reader, (010) to the right, and (100) upwards (the crystallographic directions are indicated by thin black lines). The

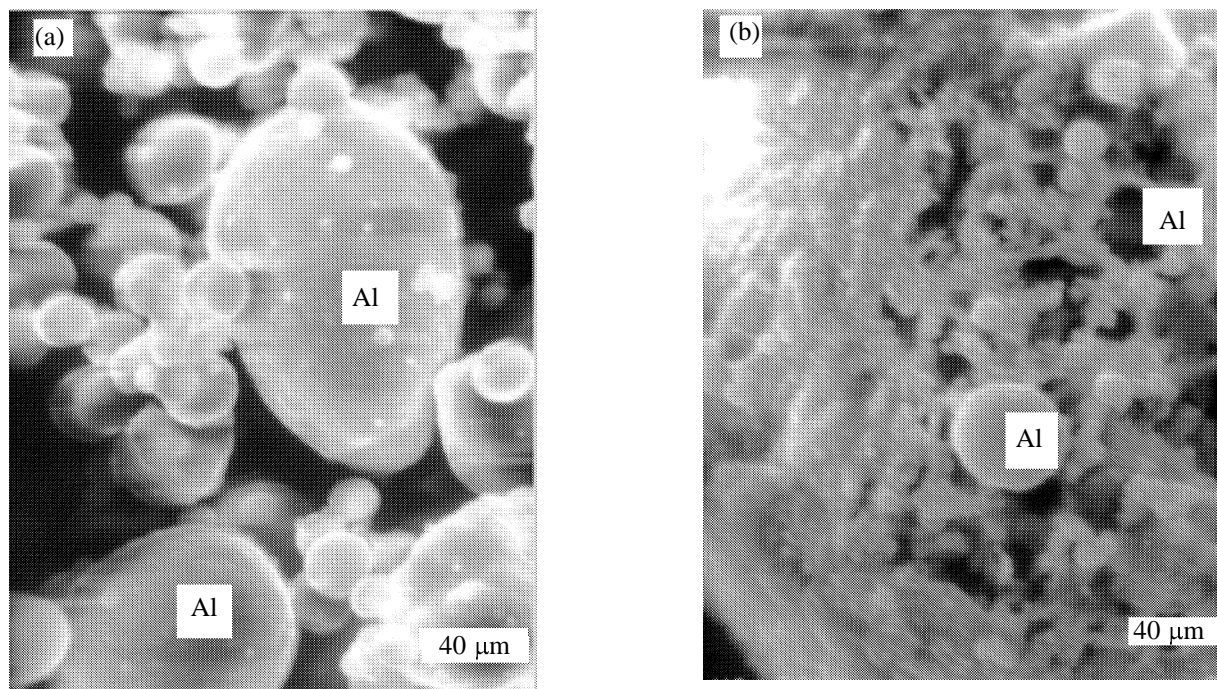


Fig. 3. Electron micrographs of particles of (a) initial Al (85 ± 15 - μm fraction) and (b) α -Fe.

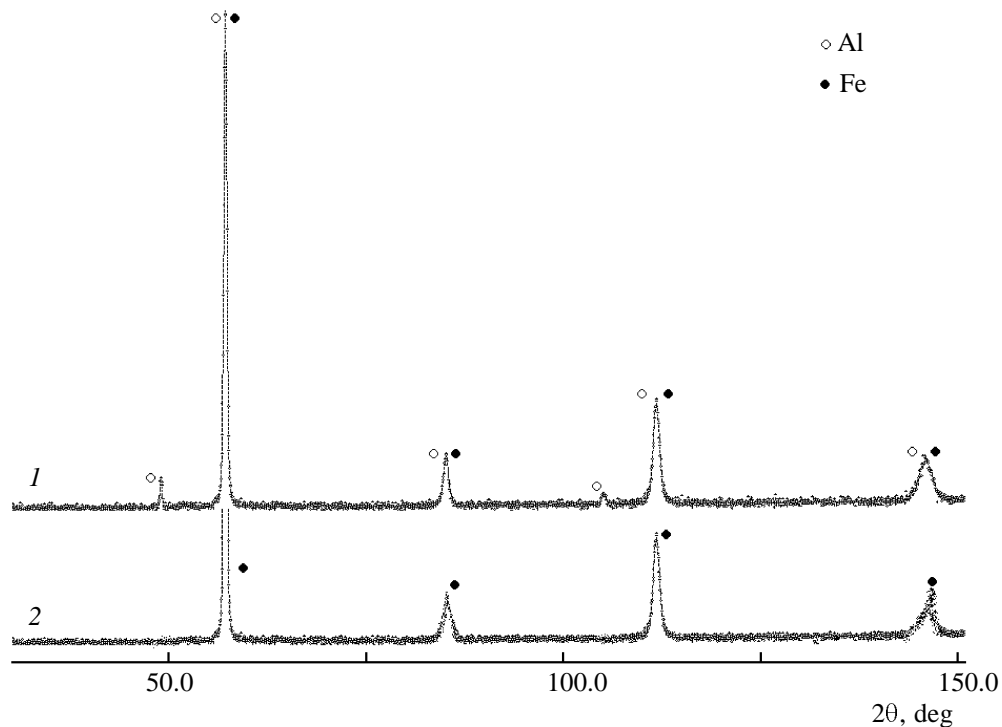


Fig. 4. Diffraction patterns of powdered iron-containing deposits obtained on a dispersed Al matrix (85 ± 15 - μm fraction): (1) immediately after Fe deposition and (2) after leaching of the residual Al. (2θ) Bragg angle.

observed deviation of the α -Fe crystallite shape from the ideal cube is due to microstresses caused by specific features of formation and growth of microcrystals of the deposit on the Al matrix.

Thus, in the reaction of a relatively concentrated (≥ 1.0 M) solution of iron(III) chloride with Al, Fe(III) is reduced to α -Fe. The reaction occurs by different mechanisms depending on the dispersity of the Al

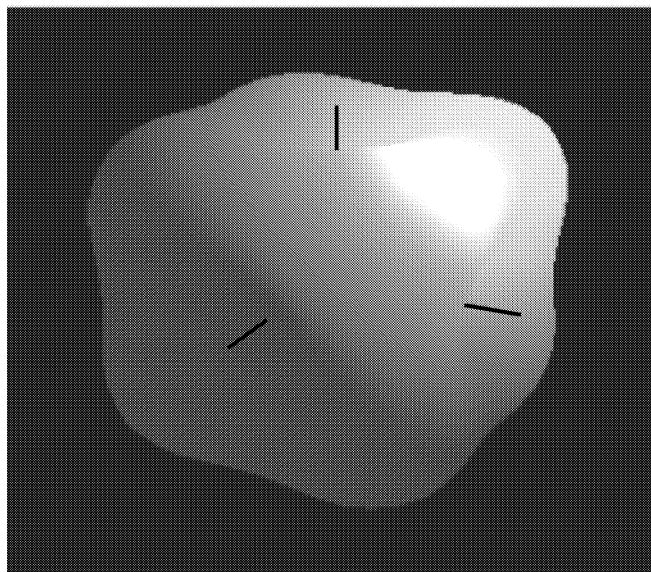


Fig. 5. Image of an α -Fe crystallite, obtained by reconstruction from X-ray diffraction data using the MAUD software.

matrix, which is confirmed by direct experiment and is satisfactorily described by the suggested model. The reduction of Fe(III) ions with Al microparticles is accompanied by the growth of the dendritic Fe deposit; the final product consists of hollow spherical particles with subnuclei on the surface and in pores.

EXPERIMENTAL

The experiment was performed with close-cut fractions of dispersed Al ($\geq 99.0\%$ purity) with the specific surface area from 63.5 (250 – 450 - μm fraction) to 258.4 cm^2 g^{-1} (71 – 100 - μm fraction), and also with A-999 Al foil (specific surface area 37.0 cm^2 g^{-1}). Analytically pure grade $\text{FeCl}_3 \times 6\text{H}_2\text{O}$ was used without additional purification as a 0.1 – 2.0 M solution. The pH was adjusted at 0.5 ± 0.02 by adding the required amounts of HCl (chemically pure grade) in the course of dilution of the stock solution. The Al : Fe molar ratio in the starting mixture was $1.5 : 1$. Experiments were performed in a temperature-controlled glass vessel equipped with an electric stirrer; the vessel was purged with prepurified Ar to remove the dissolved oxygen. Since the preliminary experiments performed with purging of the solution with an inert gas and under conditions of natural aeration showed that atmospheric oxygen did not noticeably affect the kinetics of Fe(III) reduction with Al, further experiments were performed at natural aeration. The reaction kinetics was monitored by potentiometric titration of samples taken at regular intervals {Fe(II) with bichromate and Fe(III) with a complexone, as described

in [24]}. The relative error of the indirect potentiometric determinations did not exceed 1%. The total Fe content in the solution was additionally monitored by X-ray fluorescence analysis (VRA-20L installation, Carl Zeiss). Also, samples of the initial Al and the reaction products were analyzed by X-ray phase analysis (DRON-3M diffractometer, CoK_α radiation, λ 1.79021 Å) and electron microscopy (REMMA-202M installation). The diffraction patterns were identified using the JCPDS file [25]. Prior to analysis, some deposit samples were kept in aqueous alkali to remove excess Al, washed with double-distilled water to neutral reaction and then with ethanol, and vacuum-dried at 60°C .

Also, the diffraction patterns were processed with the MAUD software [26].

The particle-size distribution of Al and Fe was determined with an Analysette C-22 laser analyzer. The measurements were performed using monochromatic radiation with λ 638 nm.

REFERENCES

1. Enzo, S., Mulas, G., Delogu, F., and Principi, G., *J. Mater. Synth. Proc.*, 2000, vol. 8, nos. 5–6, p. 313.
2. Sarkar, S. and Bansal, C., *J. Alloys Comp.*, 2002, vol. 334, no. 2, p. 135.
3. Morris, M.A. and Morris, D.G., *Mater. Sci. Forum*, 1992, vol. 88/90, no. 5, p. 529.
4. Oleszak, D., Pekata, M., Jartych, E., and Zura-wicz, J.K., *Mater. Sci. Forum*, 1997, vol. 269/272, no. 6, p. 643.
5. Grigor'eva, T.F., Barinova, A.P., and Lyakhov, N.Z., *Usp. Khim.*, 2001, vol. 70, no. 1, p. 53.
6. Zhilinskii, V.V., Lokenbakh, A.K., and Liepins, L.K., *Izv. Akad. Nauk Latv. SSR, Ser. Khim.*, 1986, no. 2, p. 151.
7. Riegel, E.R. and Schwartz, R.D., *Anal. Chem.*, 1952, vol. 24, no. 11, p. 1803.
8. Lokenbakh, A.K., Strod, V.V., and Liepins, L.K., *Izv. Akad. Nauk Latv. SSR, Ser. Khim.*, 1981, no. 1, p. 50.
9. Lyashko, A.P., Medvinskii, A.A., Savel'ev, G.G., Il'in, A.P., and Yavorovskii, N.A., *Kinet. Katal.*, 1990, vol. 31, no. 4, p. 967.
10. Dresvyannikov, A.F. and Kolpakov, M.E., *Mater. Res. Bull.*, 2002, vol. 37, no. 2, p. 291.
11. Roiter, V.A., Yuza, V.A., and Poluyan, E.S., *Zh. Fiz. Khim.*, 1939, vol. 13, no. 5, p. 605.
12. *Elektroliticheskoe osazhdenie zheleza* (Electrolytic Deposition of Iron), Zaidman, A.E., Ed., Chisinau: Shtiintsa, 1990.

13. Rozovskii, A.Ya. and Lin, G.I., *Teoreticheskie osnovy protsessa sinteza metanola* (Theoretical Foundations of Methanol Synthesis Process), Moscow: Khimiya, 1990.
14. Rozovskii, A.Ya., *Geterogennye khimicheskie reaktsii (kinetika i makrokinetika)* (Heterogeneous Chemical Reactions (Kinetics and Macrokinetics)), Moscow: Nauka, 1980.
15. Dresvyannikov, A.F. and Kolpakov, M.E., *Zh. Fiz. Khim.*, 2003, vol. 77, no. 5, p. 717.
16. Gurskii, L.I. and Zelenin, V.A., *Struktura i kinetika vzaimodeistviya metalla s okislyayushchimi sredami* (Structure and Kinetics of the Reaction of a Metal with Surrounding Media), Minsk: Vysheishaya Shkola, 1982.
17. Lokenbakh, A.K., Zaporina, N.A., and Liepins, L.K., *Izv. Akad. Nauk Latv. SSR, Ser. Khim.*, 1981, no. 1, p. 45.
18. Lokenbakh, A.K., Strod, V.V., Nekrasova, N.V., Knipele, A.Z., and Zaporina, N.A., *Izv. Akad. Nauk Latv. SSR, Ser. Khim.*, 1984, no. 5, p. 627.
19. Petrov, Yu.I., *Fiz. Tverd. Tela*, 1963, vol. 5, no. 9, p. 2461.
20. Ivanov, A.S. and Borisov, S.A., *Poverkhn. Fiz., Khim., Mekh.*, 1983, no. 10, p. 31.
21. Akimov, A.G. and Makarychev, Yu.B., *Poverkhn. Fiz., Khim., Mekh.*, 1983, no. 5, p. 88.
22. Barteneva, O.I., Bartenev, V.V., and Grigor'ev, V.P., *Elektrokhimiya*, 2000, vol. 36, no. 11, p. 1337.
23. Davydov, A.D. and Kamkin, A.N., *Elektrokhimiya*, 1978, vol. 14, no. 7, p. 979.
24. *Praktikum po fiziko-khimicheskim metodam analiza* (Practical Course of Physicochemical Methods of Analysis), Petrukhin, O.M., Ed., Moscow: Khimiya, 1987.
25. *Powder Diffraction File Inorganic Section*, Pennsylvania: Joint Committee on Powder Diffraction Standards, 1977.
26. *The Rietveld Method*, Young, R.A., Ed., New York: Oxford Univ. Press, 1993.